Colloidal processing of Pb(Zr,Ti)O₃ targets Part II – Effect of NbO₂.₅ additive

C.H. Meng, W.C.J. Wei*, J. Shieh and C.S. Chen[a]
Inst. Mat. Sci. Eng., National Taiwan University
[a]Dept. Civil Eng., National Taiwan University

Colloidal processing of $NbO_{2.5}$ and $Pb(Zr,Ti)O_3$ (PZT) powder mixtures and a study of the piezoelectric properties of sintered Nb-doped PZT (PNZT) are conducted. The PZT-based bulk samples are first prepared in various organic solvents, and then pressure-casted to form homogeneous green compacts. Results from the sedimentation and zeta (ζ)-potential measurements are used to reveal the optimum dispersive properties of PZT and $NbO_{2.5}$ colloids. High temperature dilatometry, X-ray diffractometry (XRD), scanning and transmission electron microscopy (SEM and TEM) are used to analyze the sintering, microstructures, and crystalline phases of PZT and PNZT bulk samples. The test results show that green PNZT parts with green densities higher than 4.5 g/cm³ can be sintered into high density ceramics ($\geq$ 97% theoretical density). The use of $NbO_{2.5}$ doping significantly reduces the grain growth and promotes the formation of pores. The increase in Pb vacancies and $NbO_{2.5}$ doping reduces the value of the coercive field. However, the creation of secondary phases due to over-doping degrades several important piezoelectric properties such as d_{33}, d_{31}, k_p, and P_r.

Key words: PZT, $NbO_{2.5}$, Nb-doped PZT, ζ-potential, colloids.

Introduction

Lead zirconium titanate (PZT)-based materials are promising candidates for electronic, microelectronic mechanical systems (MEMS), and non-volatile memory devices due to their superior ferroelectric and piezo-electric characteristics [1, 2]. Many aliovalent elements have been used as dopants to modify the dielectric properties of PZT. Among these elements, $NbO_{2.5}$ donor doping is reported to improve the piezoelectric proper-ties of PZT [3-5]. However, most existing studies on $NbO_{2.5}$-doped PZT simply adopt traditional powder processing techniques, and do not focus on how to optimize the sintered properties of the material.

The existing literature has pointed out that in an acidic condition, aqueous dispersion media for PZT powder will cause the dissolution of Pb in PbO [1, 7, 8], as shown in the following reactions:

$$PbO+2H^+ \longleftrightarrow Pb^{2+}+H_2O \qquad (1)$$

$$Pb(OH)_2+OH^- \longrightarrow Pb(OH)_3^+ \qquad (2)$$

The concentration of Pb^{2+} in the aqueous solution can be reduced from 100 ppm to 10^{-2} ppm by increasing the pH value from 4 to 12 [6]. Nevertheless, the dis-solution of Pb in the aqueous solution would cause a shift in the A-to-B site ratio of perovskite PZT [1, 8]. Hence, non-aqueous dispersion media are often chosen

to maintain the desired A-to-B site ratio and overcome the non-stoichiometry of Pb content in PZT.

The fabrication of fine ferroelectric ceramics by colloid processing can produce homogeneous microstructures and reliable properties [9, 10]. By adopting an organic dispersion system, the dissolution of constituents can be prevented; however, due to the low permittivities of most organic solvents, the dispersing behavior of ceramic powder in the organic system is quite different from that in the aqueous solution.

In the present study, the dispersion mechanisms of PZT and $NbO_{2.5}$ powder mixtures in three organic solvents are characterized; the green properties of the powder compacts are also measured. The electrostatic or electrosteric force between PZT colloids in the organic media is investigated in order to acquire an optimal dispersion condition for the PNZT powder mixture for the fabrication of high quality $NbO_{2.5}$-doped PZT targets.

Experimental Procedure

Materials

The ceramic powders used in the present study are PZT powder (average particle size 1.78 μm, BET surface area 1.0 m²/gm, supplied by Belltec Electronics Co. Ltd., Taiwan[1]), and $NbO_{2.5}$ powder (average particle size 1.68 μm, BET surface area 7.4 m²/gm, supplied by H.C. Starck GmbH, Germany). Selected organic solvents

*Corresponding author:
Tel : 886-2-2363-2684
Fax: 886-2-2363-4562
E-mail: wjwei@ntu.edu.tw

---

[1] According to the manufacturer's information, the supplied PZT powder already contained 1.54 mol% $NbO_{2.5}$. Therefore, the "nominal content" of $NbO_{2.5}$ is reported in this study instead of the "real content".

Table 1. Chemicals used for colloid processing

Dispersive Additive	Supplier
KD-4	
KD-5	Uniquema, ICI, England
RE-610	Rhodia Co., UK
Solvent	
Toluene (Tol)	99.5%	
Heptane (Hep)	99.5%	Acros Chemical, USA
Methyl Ethyl Ketone (MEK) 99.5%	

and dispersants for the dispersion of PZT and $NbO_{2.5}$ powders are listed in Table 1. Based on the authors' preliminary examination on the mixing of these solvents and dispersants [11], four solvent-dispersant combinations, MEK-RE610, Tol-KD4, Hep-KD4 and Hep-KD5, are identified to be the potential non-aqueous dispersion media for the PNZT powder mixture since they show better dispersive properties and a low Pb-dissolution (≤ 0.7 ppm).

In the present study, the fraction of $NbO_{2.5}$ dopant is limited to less than 10 mol%. Under this condition, it is expected that the dispersion condition for the PNZT powder mixture is similar to the condition for pure PZT powder. The concentration of $NbO_{2.5}$-doping can be calculated from the following equation:

$$NbO_{2.5} - doping(mol\%)$$
$$= \frac{2 \times [Nb_2O_5]}{2 \times [Nb_2O_5] + [Pb(Zr,Ti)O_3]} \times 100\% \quad (3)$$

Evaluation of colloidal properties

Slurries with optimum stability need to be acquired before the green bodies are consolidated under pressure casting. The preparation procedure can be divided into the following steps: first, 0.5 wt% dispersant (based on powder) is mixed with 5 vol% PNZT powder in 10 cm^3 solvent. The suspension is then mixed in a turbo-mixer (T2F, Tubula Co., Switzerland) for 18 hr with zirconia (3Y-TZP) balls as the grinding media, and then centrifuged for 20 min at 2000 rpm to measure the height ratio of the sediment and turbidity of the supernatant. Organic formulations showing better dispersing results are chosen to undergo further centrifugal sedimentation tests, for which the concentration of the dispersant is varied from 0 to 1.5 wt%. From the results of additional sedimentation testing, the optimal dispersive conditions are determined.

Dissolution of the PNZT powder mixture in various organic dispersion systems is examined by atomic absorption spectra (Analyst 800, PerkinElmer Inc., USA). Details of the analysis are reported in the authors' previous work [6]. The ζ-potential of the powder is measured by the Zeta-meter 3.0+ (Zeta-meter Inc., USA). The zeta-potential can be calculated by substitu-

ting electromobility into the Smoluchowski equation:

$$\zeta = \frac{4\pi\eta}{\varepsilon} \times u_e \quad (mV) \quad (4)$$

where η and ε are the viscosity and dielectric constant of the solvent, and u_e is the electromobility of the observed particle.

Colloidal processing and sintering

The formulation, toluene – 0.6 wt% KD4 containing 15 vol% PNZT powder, is chosen eventually for pressure casting. Details on why this formulation is selected out of the potential solvent-dispersant combinations are described in Section 3. 30 cm^3 of PNZT suspension is pressurized inside a stainless steel mold (diameter 2.6 cm and deepth 1.8 cm) with nitrogen gas at a pressure of 10 kg/cm^2 for 3 min. Upon completion, the green compacts (diameter 2.6 cm and thickness 1 cm) are removed from the mold and air-dried at room temperature for 2 days. Appropriate sintering conditions for the dried green compacts are acquired by a thermal mechanical analysis system (Setsys TMA 16/18, SETRAM Co., France). The green compacts are sintered inside an Al_2O_3 crucible containing a PZT powder bed. The sintering takes place inside a tube furnace at specified temperatures, ranging from 1000°C to 1200°C.

Characterization of sintered PNZT

The green and sintered densities of the samples are determined by the Archimedes method. Microstructural characteristics are examined under SEM and field emission SEM (XL30, Philips Co., USA, and Leo Instrument 1530, UK). The crystalline phases of the sintered PNZT are characterized by X-ray diffractometry (XRD) with Cu K_α radiation (PW1830, Philips Instrument, Netherlands). The applied voltage and current for XRD are 30 kV and 20 mA, respectively. The scanning speed is 3°/min in 0.04° steps.

The sintered bulk samples are machined into thin discs with a diameter/thickness (d/t) ratio greater than 16 (typical dimensions: 20 mm in diameter and 1 mm in thickness). The disc samples are poled and tested by a ferroelectric analyzer (TF2000, aixACT Systems GmbH, Germany) to obtain their dielectric hysteresis curves. In addition, the poled discs are tested by an impedance analyzer (4294A, Agilent Co. Ltd., USA) to acquire the frequency-dependent impedance spectrums. The piezoelectric properties of the samples are subsequently calculated from the impedance spectra using an iteration method [12].

Results and Discussion

Dispersion and consolidation

The sedimentation height ratio of the PZT slurry in the four potential dispersion systems, Tol-KD4, Hep-KD4, Hep-KD5 and MEK-RE610, is shown in Fig. 1.
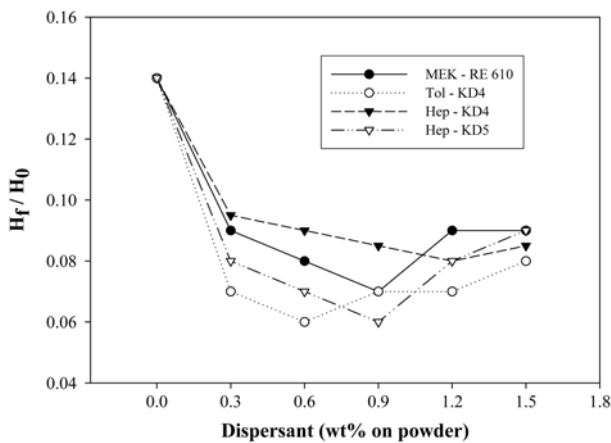
Fig. 1. Sedimentation height ratio of PZT slurry examined by centrifugal sedimentation in four solvent-dispersant systems.

It can be seen that the height ratio for each dispersion system first decreases with increasing dispersant concentration, and after reaching a minimum value; it then increases with increasing dispersant concentration. The transition point (i.e. minimum height ratio) is believed to occur at the maximum amount of dispersant that the powder surface can absorb [13, 14]. Weak flocculation between PZT particles is expected when the concentration of dispersant exceeds the saturation value of the dispersant on the powder due to either a bridging effect or particles' low ζ-potentials. It is evident from Fig. 1 that "toluene–0.6 wt% KD4" and "heptane–0.9 wt% KD5" are the two more effective solvent-dispersant systems for the dispersion of PZT powder comparing to other systems.

Figure 2(a) shows the ζ-potential of the PZT powder in the four dispersion systems. In MEK-RE610 and Tol-KD4, the PZT powder is charged and shows a positive ζ-potential on the surface, while in Hep-KD4 and Hep-KD5, the ζ-potential stays at zero at all dispersant concentrations. Nevertheless, the Hep-KD4 and Hep-KD5 systems can still offer some degree of stability according to the sedimentation results; this implies that steric force, in addition to electrostatic force, contributes to the stabilization in the two heptane-based systems. The most stable colloid system is Tol-KD4, which has the highest ζ-potential value at any particular dispersant concentration.

It is noticed that the PZT powder in MEK-RE610 is negatively charged when no dispersant is added. The charge then becomes increasingly positive as the concentration of RE610 dispersant increases. This implies that the electrons are transferred from MEK to PZT in a pure MEK medium; whereas, after RE610 is added, the electrons originally donated to PZT are now accepted by RE610. Simultaneously, electrons on the PZT surface are also accepted by RE610. As for non-polar solvents, e.g. heptane, no electron transfer is detected even with the addition of KD4 or KD5 dispersant. The Lewis acid-base strengths of these solvents are too low to
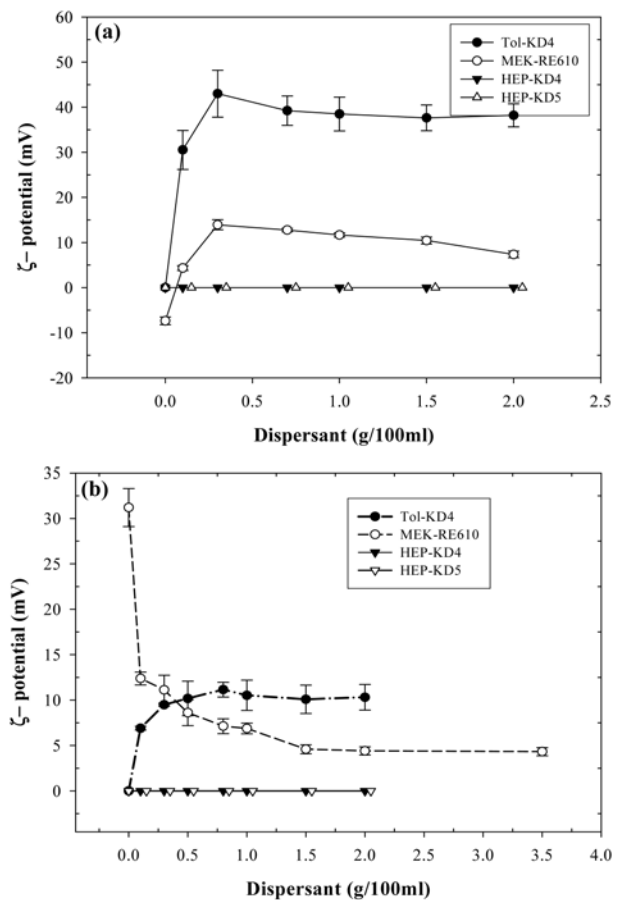

Fig. 2. Zeta-potential of (a) PZT powder, and (b) NbO₂.₅ powder in four dispersion systems at various dispersant concentrations.

donate electrons to, or accept electrons from the PZT powder [14].

In the case of Tol-KD4, the PZT powder is positively charged with the addition of KD4. It is observed that the surfaces of PZT particles stay in a neutral condition in toluene, but turn highly positive when KD4 is added. Although KD4 is capable of accepting electrons from PZT in toluene, it is believed that KD4 has a higher affinity with heptane than with the PZT powder surface. The test results reveal that the Tol-KD4 system possesses the best stability; this helps the consolidation of homogeneous green compacts during colloidal processing.

Figure 2(b) shows the ζ-potential of the NbO₂.₅ powder in the four dispersion systems chosen for this study. In the two non-polar systems, Hep-KD4 and Hep-KD5, the powder shows no surface charge. However, the NbO₂.₅ powder exhibits different charging behaviors in the MEK-RE610 and Tol-KD4 systems. The NbO₂.₅ powder is positively charged in pure MEK, which is different from the charging status of PZT powder in the same medium. By considering the isoelectric points (IEP) of PZT and NbO₂.₅ powders in aqueous solutions, the electron donority of NbO₂.₅ is seen to be stronger than that of PZT since the IEP of NbO₂.₅ is situated at a pH value of 9, which is higher than that of PZT (pH =

6). Based on the Lewis acid-base interaction, the $NbO_{2.5}$ powder will donate electrons to MEK and become positively charged, whereas the PZT powder with weak electron donor capacity will play the role of electron acceptor in MEK.

It is noticed that the $NbO_{2.5}$ powder surface remains positively charged even at high RE610 concentrations. According to one previous research, RE610 would accept electrons from the powder surface [15]. However, a contrary trend is shown in Fig. 2(b) – the positive ζ-potential decreases with increasing RE610 concentration. The dispersant RE610 can accept electrons from both $NbO_{2.5}$ and MEK due to the high basicity of these two species, and therefore, the extent of electron transfer to RE610 will be governed by the electron-donating competition between $NbO_{2.5}$ and MEK. In addition, the ζ-potential of $NbO_{2.5}$ decreases to a plateau value when the concentration of RE610 increases to more than 2.0 g/100 ml. A high concentration of RE610 tends to promote the electron donation of MEK, and therefore, the surface charging status of $NbO_{2.5}$ will eventually reach an equilibrium state (i.e. ζ-potential remains unchanged).

In the Tol-KD4 system, the highest ζ-potential of the $NbO_{2.5}$ powder is about 10 mV, which is much smaller than that of the PZT powder. In the present study, PZT is the main constituent in the suspension, and $NbO_{2.5}$ is stabilized within the PZT slurry under identical dispersive conditions. It is therefore expected that the Tol-KD4 system is still suitable for the $PZT/NbO_{2.5}$ composite system.

The green densities of the PZT samples produced from centrifugal sedimentation of various dispersing systems are shown in Fig. 3. It can be seen that the PZT green density initially increases with dispersant concentration, and then reaches the highest value when the added dispersant concentration is close to the concentration of the lowest sedimentation height ratio (i.e. around 0.6 wt%, see Fig. 1). The best green density achieved by each dispersing system is around
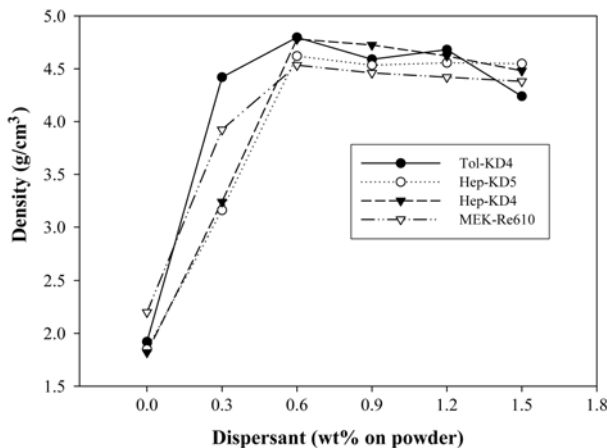
58%-61% theoretical density (T.D.). The highest green density is typically achieved when the colloidal particles are in good dispersing conditions, i.e. the slurry has the lowest sedimentation height ratio [14]. The results shown in Figs. 1 and 3 are consistent with each other. PZT samples prepared in the Tol–0.6 wt% KD4 dispersing system have the highest green densities, and therefore can be used as targets for subsequent thin film-related processing.

Densification and microstructual development

The shrinkage behavior of the PZT ceramic, produced from the Tol–0.6 wt% KD4 dispersion system, during sintering is shown in Fig. 4. The figure indicates that the shrinkage begins at 740ºC, and continues until the temperature reaches 1200ºC. The highest shrinkage rate happens at about 1150ºC. According to the study by Atkin et al. [4], the sintering behavior of PZT ceramics at temperatures between 1152ºC and 1272ºC follows the Coble model, which explains the intermediate and final stages of sintering, typically governed by volume diffusion. Figure 5 shows the densities and average grain sizes of the sintered PZT ceramics at four sintering temperatures. These samples are produced from the
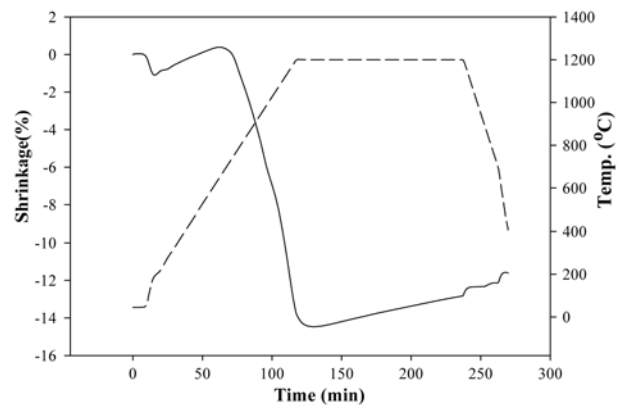

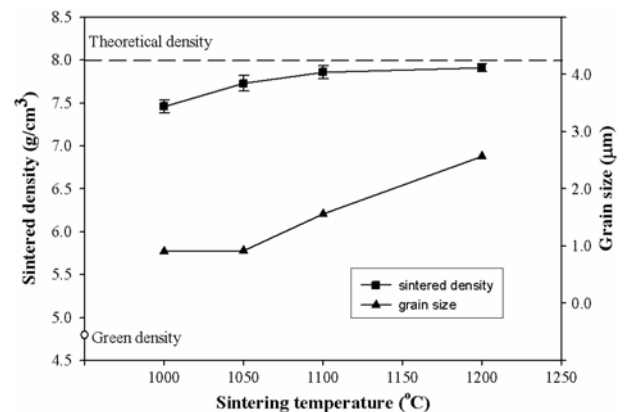**Fig. 4.** Dilatometric shrinkage of the PZT ceramic, produced from Tol–0.6 wt% KD4, during sintering.

Fig. 3. Green densities of PZT samples produced from centrifugal sedimentation of various dispersing systems.

Fig. 5. Sintered densities and average grain sizes of PZT ceramics, produced from Tol–0.6 wt% KD4, at various sintering temperatures.
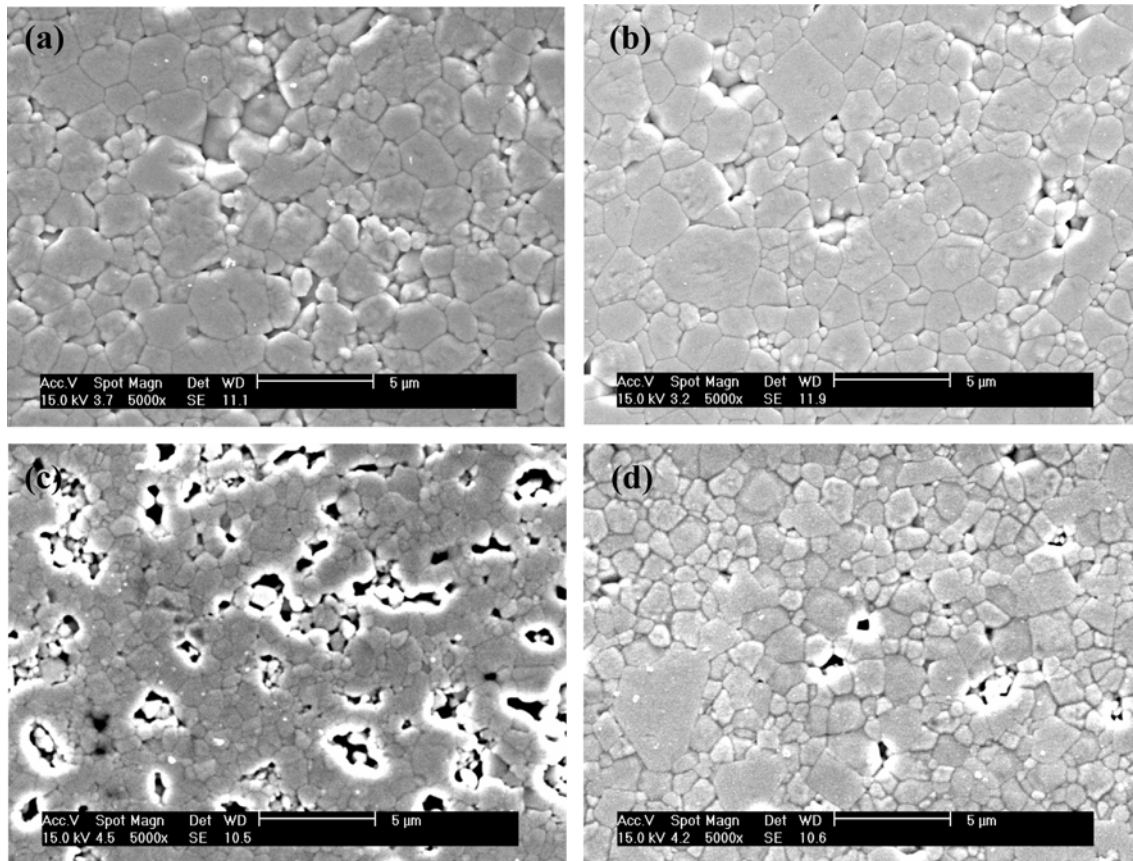
Fig. 6. SEM micrographs of sintered PZT (1200°C, 1 hr) doped with (a) 1 mol%, (b) 2 mol%, (c) 4.7 mol%, and (d) 9.4 mol% $NbO_{2.5}$.

Tol–0.6 wt% KD4 dispersion system. It is evident from Fig. 5 that the sintered density increases with temperature and reaches a value of 7.92 g/cm³ at 1200°C. At relatively low sintering temperatures (i.e. 1000°C and 1050°C), no noticeable grain growth is observed. However, the grain size is more than doubled when the sintering temperature reaches 1200°C. The present of large abnormal grains is detected in samples sintered at temperatures higher than 1200°C.
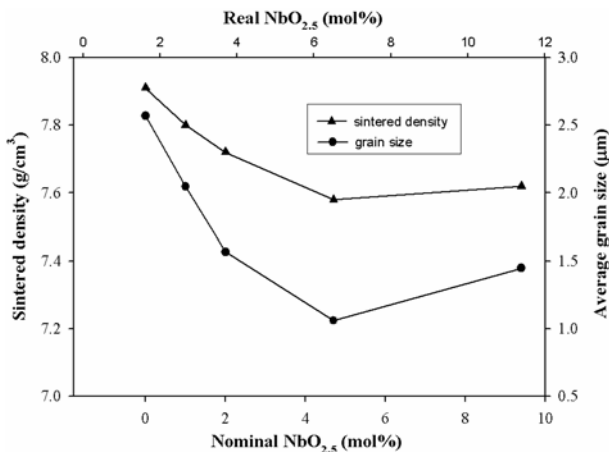

Fig. 7. Grain sizes and densities of sintered PZT ceramics (1200°C, 1 hr) with various nominal $NbO_{2.5}$ doping amounts.

SEM micrographs of the PZT ceramics doped with various amounts of $NbO_{2.5}$ are shown in Fig. 6. The densities and grain sizes of these $NbO_{2.5}$-doped PZT ceramics are shown in Fig. 7. It can be seen that the bulk density decreases to a minimum value (i.e. 7.48 g/cm³) when the nominal doping amount of $NbO_{2.5}$ increases to 4.7 mol% (i.e. real concentration of 6.2 mol%). Some existing studies have shown that the density of PNZT can be greater than that of pure PZT when the $NbO_{2.5}$ doping concentration is below 1.8 mol% [5, 16].

Phase and piezoelectric properties

Fig. 8 shows the XRD patterns for various PNZT ceramics sintered at 1200°C for 1 h. When the $NbO_{2.5}$ doping level is below 5 mol%, the crystalline phase of PNZT indicates a tetragonal structure. Above this doping level, two additional peaks appear at 29.24° and 58.76°; these belong to the cubic phase of $Pb_2Nb_{1.33}Ti_{0.66}O_{6.66}$. As the amount of $NbO_{2.5}$ reaches 9.4 mol%, another group of new peaks, belonging to the cubic $Pb_2(Nb_{0.67}Ti_{0.33})_2O_{6.66}$ phase, appears.

Figure 9 shows the hysteresis curves for PZT doped with 0, 2, 4 and 9 mol% $NbO_{2.5}$[2]. The coercive fields

---

[2]In the present study, PZT doped with 0, 2, 4 and 9 mol% $NbO_{2.5}$ are represented by PNZT-0, PNZT-2, PNZT-4 and PNZT-9, respectively.
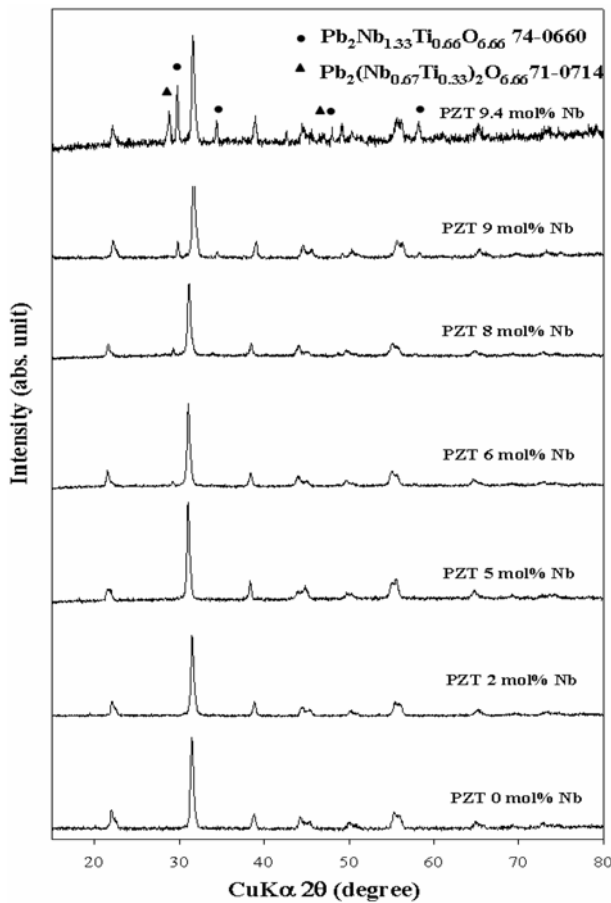
Fig. 8. XRD patterns for various PNZT ceramics sintered at 1200°C for 1 h.

Fig. 9. Dielectric hysteresis curves for various PNZT ceramics.

becomes larger with smaller grains, would degrade PZT's ferroelectric characteristics [17]. In other words, PZT ceramics with smaller grains are likely to exhibit smaller remanent polarizations, larger coercive fields, and lower electromechanical coupling factors and piezoelectric coefficients. On the contrary, the present study shows that the coercive field remains small even with small grain sizes. It is therefore concluded that the variation of the coercive field relies heavily on the amount of Pb vacancies (i.e. concentration of $NbO_{2.5}$ doping), whereas the permanent polarization is more susceptible to the change in grain size.

The experimental data in Table 2 show that the softening effect originally anticipated from $NbO_{2.5}$ doping is hampered by small grain sizes. As stated previously, the depolarization field created by the space charge effect is higher when the grains become smaller [17]; this would lower the poling efficiency and remanent polarization, and subsequently promote the aging in ferroelectric ceramics. The space charge effect is therefore one of the dominate factors which influences the piezoelectric properties of the PNZT ceramics prepared in the current study. The present study suggests that the main factors, which affect the ferroelectric and piezoelectric properties of $NbO_{2.5}$-doped PZT, are the grain

(E_c) are 1.52, 1.36 and 1.18 MV/m for PNZT-0, PNZT-2 and PNZT-4, respectively. The evolution of the hysteresis behaviour with respect to the doping level of $NbO_{2.5}$ is evident. When the concentration of the $NbO_{2.5}$ doping increases, the coercive strength decreases. However, as the concentration of the $NbO_{2.5}$ doping increases to 9 mol%, the coercive field value increases to more than 2.0 MV/m. The remanent polarizations (P_r) are 0.36, 0.17, 0.13 and 0.16 C/m² for PZT samples doped with 0, 2, 4 and 9 mol% $NbO_{2.5}$, respectively. When the $NbO_{2.5}$ doping concentration is below the solubility limit (around 6.5 mol %), the decrease in the coercive field obeys the typical softening effect, commonly found in donor-doped PZT ceramics. It is evident from the SEM images that the increase in $NbO_{2.5}$ doping concentration would inhibit grain growth and induce porosity (see Fig. 6), and therefore, apart from the softening effect induced by the Pb vacancies, the adverse ferroelectric characteristics caused by smaller grain sizes would also have to be considered in the evolution of the dielectric hysteresis curve.

The piezoelectric properties of the PNZT ceramics produced from the Tol–0.6 wt% KD4 dispersion system are summarized in Table 2. Okazaki and Nagata reported that the space charge-related electrical field, which
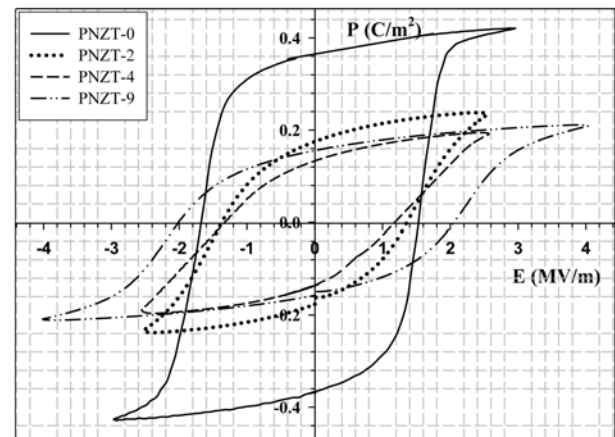
Table 2. Piezoelectric properties of PNZT ceramics

	PNZT-0	PNZT-2	PNZT-4	PNZT-9
Grain Size (μm)	2.57	1.57	1.27	1.42
P_r (C/m²)	0.36	0.17	0.13	0.16
E_c (MV/m)	1.52	1.36	1.18	2.05
k_p	0.52	0.3	0.28	0.15
k_t	0.51	0.26	0.26	0.13
d_{31}(pC/N)	-91.43	-51.35	-50.45	-23.89
d_{33} (pC/N)	95.35	-	-	-
Dielectric Constnat K	979	957	992	719

Note: In the present study, PZT doped with 0, 2, 4 and 9 mol% $NbO_{2.5}$ are represented by PNZT-0, PNZT-2, PNZT-4 and PNZT-9, respectively.

size, $NbO_{2.5}$ doping concentration, and existence of second phases. By looking at the measured data for the PNZT-9 ceramic in Table 2, it is evident that the existence of second phases heavily degrades the ceramic's piezoelectric characteristics. To obtain excellent piezoelectric properties, the amount of $NbO_{2.5}$ doping should be kept low to prevent the reduction in grain size and the promotion of second phases.

Conclusions

Dense and homogeneous $NbO_{2.5}$ doped-PZT targets are successfully synthesized by colloidal processing. Comparing to other complex oxide sintering procedures, the colloid method described in the present study is capable of fabricating denser PZT and PNZT targets. The design and control of the dispersion system in colloidal processing are essential for the production of high quality $NbO_{2.5}$-doped PZT targets. This study shows that the toluene solvent system with 0.6 wt% KD4 dispersant shows excellent dispersing and particle packing characteristics for the $PZT/NbO_{2.5}$ powder mixture based on the centrifugal sedimentation, ζ-potential, and green density tests. Studies of the ζ-potentials of the PZT and PNZT particles in various solvent-dispersant systems reveal the stabilizing mechanism. In the Hep-KD4 and Hep-KD5 systems, steric hindrance is the main stabilization mechanism for the colloids, whereas in the Tol-KD4 and MEK-RE610 systems, electrosteric hindrance is the stabilizing basis.

The bulk $NbO_{2.5}$-doped PZT samples sintered at 1200ºC for 1 h are able to achieve a density better than 97.6% T.D. XRD patterns for the PNZT bulk ceramics suggest that the solubility limit of $NbO_{2.5}$ in PZT is approximately 6.5 mol% (including the initial amount of $NbO_{2.5}$ contained within the PZT powder supplied). The correlation between piezoelectric performance and microstructure indicates the existence of pyrochloric phases when the amount of $NbO_{2.5}$ doping exceeds the solubility limit. The formation of pores and smaller grains due to $NbO_{2.5}$ doping causes a decrease in d_{33}, d_{31}, k_p and P_r. E_c decrease with increasing Pb vacancies (i.e. increasing $NbO_{2.5}$ concentration). When the doping level of $NbO_{2.5}$ is below 2 mol%, the softening effect is optimized with a satisfactory grain size and porosity level.

References

1. K. Uchino, S. Nomura, L.E. Cross, R.E. Newnham and S.J. Jang, J. Mater. Sci. 16 (1981) 569-578.
2. B. Noheda, J.A. Gonzalo, L.E. Cross, R. Guo, S.E. Park, D.E. Cox, and G. Shirane, Phys. Rev. B 61 (2000) 8687-8695.
3. T. Ikeda, Y. Tanaka, T. Ayakawa, and H. Noake, Jpn. J. Appl. Phy. 3[10] (1964) 581-587.
4. R.B. Atkin, R.L. Holman, and R.M. Fulrath, J. Am. Ceram. Soc. 54 (1971) 113-115.
5. M. Pereira, A.G. Peixoto, and M.J.M. Gomes, J. Europ. Ceram. Soc. 21 (2001) 1353-1356.
6. B.Y. Yu, W.T. Hsu, and W.C.J. Wei, (2/2006) accepted by J. Ceram. Proc. Research.
7. D.R. Lide (editor), Hand book of Chemistry and Physics, 72nd ed. (1991).
8. X.Y. Wang, S.W. Lu, B.I. Lee, and Larry A. Mann, Mater. Res. Bull. 35 (2000) 2555-2563.
9. K.C. Hsu, K.L. Ying, L.P. Chen, B.Y. Yu, and W.J. Wei, J. Am. Ceram. Soc. 88[3] (2005) 524-529.
10. B.Y. Yu, W.J. Wei, and K.C. Hsu, J. Ceram. Proc. Research 5[2] (2004) 163-170.
11. C.H. Meng, Analysis on processing and properties of Na₂O₅-doped PZT targets and thin films, National Taiwan University M.Sc. Thesis (2005).
12. M. Alguero, C. Alemany, and L. Pardo, J. Am. Ceram. Soc. 87 (2004) 209-215.
13. Y. Tomita, L.C. Guo, N. Uchida, and K. Uematsu, J. Am. Ceram. Soc. 78 (1955) 2153-2156.
14. F.W. Fowkes, Acid-base Interactions: Relevance to Adhesion Science and Technology, VSP, Utrecht, The Netherlands (1991) 93-115.
15. T. Chartier and E. Jorge, J. Europ. Ceram. Soc. 11 (1993) 387-393.
16. M. Hammer and M.J. Hoffmann, J. Am. Ceram. Soc. 81 (1998) 3277-3284.
17. K. Okazaki and K. Nagata, J. Am. Ceram. Soc. 56 (1973) 82-86.